Available online at www.sciencedirect.com
ScienceDirect
ISPRS Journal of Photogrammetry & Remote Sensing 63 (2008) 84–98
PHOTOGRAMMETRY & REMOTE SENSING
www.elsevier.com/locate/isprsjprs

Unsupervised robust planar segmentation of terrestrial laser scanner point clouds based on fuzzy clustering methods

Josep Miquel Biosca, José Luis Lerma *

Polytechnic University of Valencia, Department of Cartographic Engineering, Geodesy and Photogrammetry, C° de Vera s/n, Building 7i, 46022 Valencia, Spain

Received 30 November 2006; received in revised form 18 July 2007; accepted 20 July 2007
Available online 19 September 2007

Abstract

Terrestrial laser scanning is becoming a common surveying technique to measure quickly and accurately dense point clouds in 3-D. It simplifies measurement tasks on site. However, the massive volume of 3-D point measurements presents a challenge not only because of acquisition time and management of huge volumes of data, but also because of processing limitations on PCs. Raw laser scanner point clouds require a great deal of processing before final products can be derived. Thus, segmentation becomes an essential step whenever grouping of points with common attributes is required, and it is necessary for applications requiring the labelling of point clouds, surface extraction and classification into homogeneous areas. Segmentation algorithms can be classified as surface growing algorithms or clustering algorithms. This paper presents an unsupervised robust clustering approach based on fuzzy methods. Fuzzy parameters are analysed to adapt the unsupervised clustering methods to segmentation of laser scanner data. Both the Fuzzy C-Means (FCM) algorithm and the Possibilistic C-Means (PCM) mode-seeking algorithm are reviewed and used in combination with a similarity-driven cluster merging method. They constitute the kernel of the unsupervised fuzzy clustering method presented herein. It is applied to three point clouds acquired with different terrestrial laser scanners and scenarios: the first is an artificial (synthetic) data set that simulates a structure with different planar blocks; the second a composition of three metric ceramic gauge blocks (Grade 0, flatness tolerance ±0.1 μm) recorded with a Konica Minolta Vivid 9i optical triangulation digitizer; the last is an outdoor data set that comes up to a modern architectural building collected from the centre of an open square. The amplitude-modulated-continuous-wave (AMCW) terrestrial laser scanner system, the Faro 880, was used for the acquisition of the latter data set. Experimental analyses of the results from the proposed unsupervised planar segmentation process are shown to be promising.

Keywords: Laser scanning; Segmentation; Fuzzy clustering; Algorithms; Point cloud

1. Introduction

A terrestrial laser scanner is a powerful surveying tool used to measure quickly and accurately dense point clouds. This tool fulfils the requirements of high density of data, speed of acquisition and accuracy in different fields, such as industrial design, civil engineering, cultural heritage, telecommunications, medicine, and, last but not least, multimedia environments. Furthermore, point cloud data sets allow producers to analyse complex as-built constructions, and deepen reverse engineering and quality

* Corresponding author. Tel.: +34 96 3877550; fax: +34 96 3877559.
E-mail address: jllerma@cgf.upv.es (J.L. Lerma).

0924-2716/$ - see front matter © 2007 International Society for Photogrammetry and Remote Sensing, Inc. (ISPRS). Published by Elsevier B.V. All rights reserved.
doi:10.1016/j.isprsjprs.2007.07.010

control for industrial applications. Two of the main concerns to build up a complete 3-D model are both accuracy and occlusions, and should be carefully considered for planning purposes. The idea of both complete and massive 3-D point measurements is sometimes a challenge in terms of data acquisition and processing. This is particularly true when dealing with the documentation of scenes with complex relief or intricate detail.

Raw laser scanner point clouds require a great deal of processing before final products can be derived. The capability of carrying out useful analyses is rather limited with unstructured 3-D points. Thus, segmentation becomes an essential step whenever grouping of points with common attributes is required. Segmentation itself is one of the main research areas in the laser scanning field not only because of the requirement of introducing some level of organization into the data before extraction of effective information (Filin and Pfeifer, 2005), but also because it is one of the main processing steps far from being solved even for planar features (Hoover et al., 1995). The literature is full of both research papers and projects dealing with segmentation. The purpose of segmentation is usually different in the computer vision community compared to the photogrammetric community. The former are more concerned with segmentation algorithms and performance evaluations (Hoffman and Jain, 1987; Besl, 1988; Hoover et al., 1995; Hoover et al., 1996; Jiang et al., 2000; Osorio et al., 2005) and deal mainly with regular flat and smooth-shaped objects and industrial pieces. The latter frequently tackle more complex shapes representing a gamut of both natural and man-made phenomena for surveying purposes. Regarding the airborne laser scanner data, most of the experts deal with segmentation either to extract 3-D features such as buildings (Rottensteiner and Briese, 2003; Matikainen et al., 2004; Filin and Pfeifer, 2005) and bridges (Sithole and Vosselman, 2006) or to reconstruct 3-D city models (Haala and Brenner, 1999; Maas and Vosselman, 1999; Takase et al., 2003). Segmentation in the field of terrestrial laser scanning has an additional problem to overcome, namely to work with fully 3-D data instead of 2 1/2D data (Belton and Lichti, 2006). Rabbani et al. (2006) reviewed some segmentation problems when processing industrial point clouds such as handling curved objects or finding the best segmentation parameters, especially when there are a large number of them.

Some algorithms are known in literature for segmenting laser scanner point clouds into planar regions. They can be classified into two categories: region growing (Hofmann et al., 2002; Dold and Brenner, 2004; Pu and Vosselman, 2006) and clustering (Filin, 2002; Hofmann, 2004; Filin and Pfeifer, 2005, 2006). For more general region types i.e. quadratic or polynomial patches, the nature of algorithms can be extended (Hoover et al., 1996). Planar patches are the most general regions used to segment both indoor and outdoor data for several reasons: first, they can be modelled and determined easily following different approaches; second, most of the man-made environments, objects and features are flat, or can be decomposed into piecewise planar patches (Bartoli, 2001). Lerma and Biosca (2005) tested a segmentation algorithm based on both region growing and clustering methods on a historic building for two different purposes: to classify point clouds depending on roughness, and to extract boundaries on planar features. Segmentation examples of planar patches for the aforementioned categories can be extensively found in terrestrial as well as aerial surveying applications.

Surface growing algorithms are generally used in point cloud segmentations due to their easy implementation and speed. However, they suffer the problem of seed choice. If they lie on a discontinuity, problems can occur. Moreover, different choices of seed may result in different segmentation outputs. Consequently, region growing algorithms can not be considered as robust segmentation algorithms. On the other hand, several aggregating criteria are used: proximity of points, locally planar and smooth normal vector field (Vosselman et al., 2004). However, there is no universal criterion valid for any case.

Clustering, and more specifically fuzzy clustering methods, are powerful tools to detect clusters in feature spaces. Since all the points lying on the same surface have similar features, i.e. curvature, they create a dense region in a feature space. Thus, clustering methods are a useful tool to extract surfaces from point clouds. Filin (2002) proposed a feature-based space in which each point is represented by a feature vector with seven parameters. Clusters can be identified after grouping points in the feature space by proximity. Hofmann (2004) focused the previous clustering method to a feature vector with three parameters for each triangle of a TIN-structure. Filin and Pfeifer (2005, 2006) suggested an adaptive neighbourhood system based on a distance criteria and the geometrical content of the data (measured points). All these clustering algorithms were presented for segmentation of airborne laser scanning.

The paper presented herein follows the clustering method proposed by Filin (2002), reviews fuzzy clustering algorithms and shows their ability to perform a robust segmentation for terrestrial laser scanner point clouds. The rest of the paper is organized as follows: Section 2 presents the fuzzy clustering segmentation algorithm method used to categorize point clouds, while

Section 3 reports on three experiments conducted to evaluate our proposed fuzzy-based clustering segmentation algorithm on different scenarios: the first is a simulated (synthetic) 3-D target; the second a controlled indoor target composed of three metric gauge blocks; and the third an outdoor survey of a modern architectural building. The terrestrial laser scanner systems selected to conduct the experiments operate by optical triangulation and phase difference methods, for the second and third experiments, respectively; for the first, the synthetic data is computed considering either a time-of-flight or a phase difference system. Therefore, it can be tested whether the methodology proposed is independent of both scanner system and scale or not.

2. Fuzzy clustering segmentation method

Segmentation is understood as the process of splitting data into disjoint regions that maintain both unique and homogeneous features from their surroundings. Therefore, segmentation can be considered as a labelling process to classify data according to the region it belongs to. The process has the following steps: first, classification of data points into surface categories; second, classification of points lying on planar features into different planes; third, refinement of planar surfaces; and forth, validation. Each step will be explained in the following subsections. As each point is going to be represented in a feature space to perform the fuzzy clustering segmentation, this section starts with a definition of the feature space.

2.1. Feature space

Each feature vector (associated with a 3-D point) should model the main characteristics of its nearby region. Regions are extracted after locating maxima in feature space. Thus, the higher dense zones of this space should represent the main surfaces in object space. A feature vector is composed of three attributes: $(h_i, \overrightarrow{n_i}, d_i)$, where h_i is the height difference of a point relative to its neighbours, $\overrightarrow{n_i}$ is the unit normal vector of the tangent plane, and d_i is the distance of the tangent plane to the origin. The height difference h_i is computed as the distance from the point to the best fitting plane to its neighbours along the normal direction. Thus, if the fitting plane is horizontal, h_i is the vertical distance from the point to the plane. On the contrary, if the fitting plane is vertical, h_i is the horizontal distance from the point to the plane. It is mandatory to compute both h_i and $\overrightarrow{n_i}$ to select r_i, maximum allowed distance from a point to its neighbourhood.

The height of a point to its neighbours, h_i, is commonly used to measure local variations. It provides an indication of the kind of surface where the point is: low values will correspond to points lying on planar surfaces, while higher values will indicate grades of undulation. Additionally, h_i can be used as an edge detector. A unit normal vector, $\overrightarrow{n_i} = (n_1, n_2, n_3)$, is computed as the median of a set of unit normal vectors. Several unit normal vectors $\overrightarrow{n_{jk}}$ are calculated for a single point i following the equation:

$$\overrightarrow{n_{jk}} = \frac{\overrightarrow{v_{ij}} \times \overrightarrow{v_{ik}}}{|\overrightarrow{v_{ij}} \times \overrightarrow{v_{ik}}|} \tag{1}$$

where $\overrightarrow{v_{ij}}$ and $\overrightarrow{v_{ik}}$ are vector differences of the nearby points j and k in respect to point i. As the median of the unit normal vectors has not to be unitary, it must be normalised. Avoiding opposite directions for similar surfaces is controlled by the scalar product of two normal vectors. If $\overrightarrow{n_a} \cdot \overrightarrow{n_b} \approx -1$ (where a and b represent planes with similar slopes), the normal vector directions are opposite and one must be changed mathematically. Once the normal vector of the tangent plane is known, the distance of that plane to the origin is computed by means of:

$$d_i = -n_1 x_i - n_2 y_i - n_3 z_i \tag{2}$$

h_i is expressed with the unit of the point coordinates, ranging from 0 to ∞. The components of the normal vector range from -1 to 1 and they have no dimensions. Finally, the distance from the tangent plane to the origin, d_i, is also expressed with the unit of the point coordinates, but it ranges from $-\infty$ to $+\infty$.

2.2. Classifying points fitting on planar surfaces

In order to perform a planar segmentation of a point cloud, the first step is to extract all the points lying on planar surfaces. In other words, we must classify (tag) points according to whether they lie on planar surfaces or not. For this purpose, h_i can be used to define different classes. Surface classes will exist within the point neighbourhood. For homogeneous point densities as well as homogeneous levels of noise on every surface, h_i will be around zero if a point is on a planar region and there is no discontinuity in its neighbourhood. However, if a point is on a curved surface, the distance from that point to the best fitting plane will be greater than zero. In addition, if there is a discontinuity inside the neighbourhood, the nearer the discontinuity is to the point, the higher h_i will be. Moreover, if there is more than one discontinuity near a point, h_i will increase. A priori, height differences are good estimates to classify not only points belonging to planar surfaces but also cluster points into a

set of classes. In general, classes will represent surface categories, ranging from flat surface up to rough or edge. For instance, typical data sets contain four categories: planar surface, smooth undulation, high undulation and edge. Each class in the object space generates a dense region in the feature space.

Fuzzy clustering methods such as the Fuzzy C-Means (FCM) algorithm defined by Bezdek (1981) have the ability to detect clusters in large data sets without any initialization (they can be randomly set), in contrast to traditional clustering methods. This means that there is no need to either use sample points or define cluster centroids. FCM algorithm finds the final prototypes that correspond to the clusters in the data by minimizing the objective function (also known in the literature as cost function):

$$J(X,C,U)=\sum_{i=1}^{c}\sum_{j=1}^{n}u_{ij}^{m}\left\|x_j-c_i\right\|^2 \tag{3}$$

where $X=\{x_1, x_2,\ldots, x_n\}$ symbolizes the data, in our case, the height differences h_i, $C=\{c_1, c_2,\ldots, c_c\}$ the prototypes of the clusters $\{P_1, P_2,\ldots, P_c\}$, and $U=[u_{ij}]$ is a $c\times n$ matrix, called the fuzzy C-partition matrix, that satisfies the following conditions:

$$\begin{aligned} &u_{ij}\in[0,1] \text{ for all } i \text{ and } j\\ &0<\sum_{j=1}^{N}u_{ij}<N \text{ for all } i\\ &\sum_{i=1}^{C}u_{ij}=1 \text{ for all } j \end{aligned} \tag{4}$$

where u_{ij} is the grade of membership of a point x_j into cluster c_i, $m\in[1,\infty)$ is a weighting exponent called the fuzzifier, and $\|x_j-c_i\|$ is the distance of the point x_j to the prototype c_i. A value of m equal to 2 is frequently recommended in the literature, being the solution rather insensitive to differences of a few units. Fuzzy partitioning is carried out through an iterative optimization of the objective function updating memberships u_{ij} and prototypes c_j by:

$$u_{ij}=\frac{1}{\sum_{k=1}^{N}\left(\frac{\|x_j-c_i\|}{\|x_j-c_k\|}\right)^{\frac{2}{m-1}}} \tag{5}$$

$$c_i=\frac{\sum_{j=1}^{N}u_{ij}^{m}x_j}{\sum_{j=1}^{N}u_{ij}^{m}}. \tag{6}$$

This iteration will stop after satisfying the condition: $|J^{(k-1)}-J^{(k)}|<\varepsilon$, where ε is a positive number and k is the number of iterations. This procedure converges to a local minimum. As a result, prototypes are placed the closest to the data nucleus, and, at the same time, as far from the others as possible.

The number of surface categories must be estimated for each data set. They set up the number of surfaces that will exist in the area of a neighbourhood. It has been proved that three surface categories are appropriate for most of the objects. However, if an object has a curved surface with a radius larger than the neighbourhood radius, a minimum of four categories will be required for a good classification. Fig. 1 shows the classification effects on two data sets (the first, Fig. 1a and Fig. 1b; the second, Fig. 1c and Fig. 1d) when the number of surface

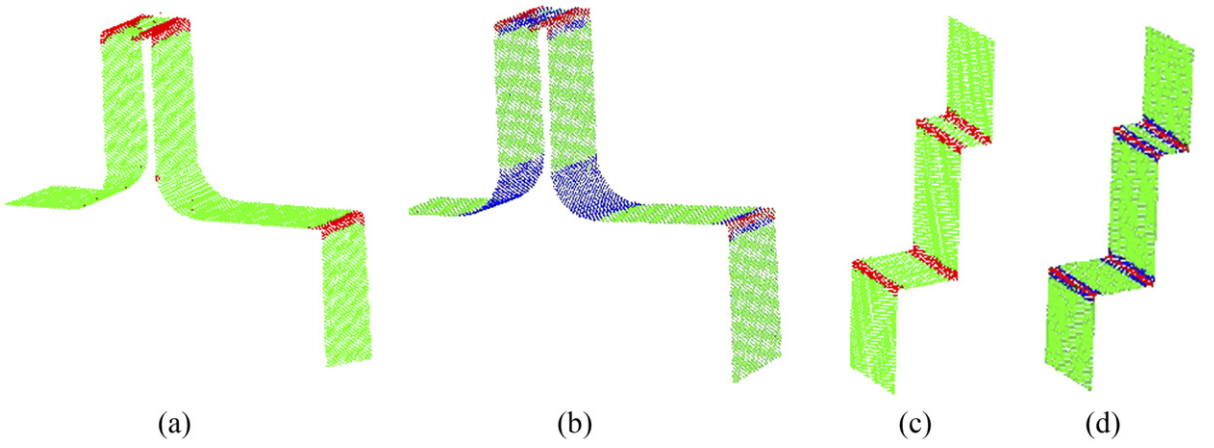

Fig. 1. (a, c) Point clouds classified into two surface categories: planar; and, undulated surfaces or edges. (b, d) Point clouds classified into three surface categories: planar; smooth undulation; and, undulated or edges.

categories is both under- and over-determined, respectively. When the first data set is classified into two categories, some curved regions are classified as planar surfaces (Fig. 1a). However, when it is classified into three categories, the point cloud is correctly classified (Fig. 1b). Regarding the second set of points, two categories are enough to classify correctly the point cloud (Fig. 1c). It should be noted that over-determination with three categories also leads to correct results (Fig. 1d).

Once the prototypes of the classes and the fuzzy C-partition matrix $U=[u_{ij}]$ are known, it is possible to classify data after checking maximum membership u_{ij} between each data point j and class i. In addition, this procedure performs as an outlier detector due to noisy points in planar regions being classified as points on a curved surface.

The chance to find a discontinuity inside a neighbourhood increases with its size. Thus, points lying on planar surfaces close to edges will not be classified as a planar surface and will be excluded to compute planar surfaces. However, this effect will be corrected afterwards in the refinement step. Therefore, the sensitivity of the method regarding r is low.

2.3. Extracting planar surfaces

The next step in the segmentation process is to extract the different planar surfaces from points classified as planar surface (Section 2.2). The most common way to represent a plane is by means of the explicit equation:

$$z = a \cdot x + b \cdot y + c. \tag{7}$$

However, Eq. (7) is not valid for terrestrial laser scanner applications because it fails when dealing with vertical planes. In order to overcome this situation, the implicit plane equation (Eq. (8)) can be used:

$$Ax + By + Cz + D = 0 \tag{8}$$

where (A,B,C) are the normal vector components and D is the distance to the origin (0,0,0).

It is possible to obtain the parameters for all the planar surfaces locating the maxima in the feature subspace $(\overrightarrow{n}, d) = (A, B, C, D)$, created with the whole set of points belonging to the planar category. If the number of planes in the data set was a priori known, we could achieve this aim by means of the FCM algorithm. As most of the times it is difficult to define beforehand the number of planar surfaces in a point cloud, the Possibilistic C-Means (PCM) mode-seeking algorithm is used to solve this problem.

PCM is a modification of the FCM algorithm developed by Krishnapuram and Keller (1993, 1996) that casts the clustering problem into the framework of possibility theory. It is able to detect the data structure (number of classes and prototypes) without defining its number of classes. The new objective function to minimize is proposed as follows:

$$J(X, C, U) = \sum_{i=1}^{C} \sum_{j=1}^{N} u_{ij}^{m} \left\| x_j - c_i \right\|^2 + \sum_{i=1}^{C} \eta_i \sum_{j=1}^{N} \left(1 - u_{ij}\right)^m \tag{9}$$

where η_i is a positive number (scale parameter) related to the size of the cluster. This value defines the distance at which the membership value of a point in a cluster becomes 0.5. It has to be chosen depending on the desired "bandwidth" of the membership distribution. Krishnapuram and Keller (1993, 1996) proposed different ways to estimate η_i. Following their suggestions, a value of m equal to 1.5 is selected. After our experiences, the larger the m value, the lower the chance to detect small clusters, being the PCM algorithm more sensitive to variations of m than the FCM algorithm.

The new membership equation after differentiating Eq. (9) with regard to u_{ij} and setting it to 0 is:

$$u_{ij} = \frac{1}{1 + \left(\frac{\left\|x_j - c_i\right\|^2}{\eta_i}\right)^{\frac{1}{m-1}}}. \tag{10}$$

Prototypes are computed as in the FCM algorithm. The objective function is iteratively minimized until the completion criterion is reached. After iterations, prototypes get the coordinate values of the centres of good clusters in the data set. It is understood that a *good* cluster fits perfectly a dense region. The FCM finds a fuzzy C-partition of a given data set regardless of the number of clusters that actually exists in the data set. Thus, each prototype may or may not correspond to a dense region. On the contrary, prototypes provided by the PCM algorithm fit actual dense regions. If the defined number of classes, C, is less than the true number of classes in the data set, C_0, the PCM algorithm finds C good clusters, despite its reduced number. If C is greater than C_0, some of the resultant prototypes will be identical and there will be only C_0 different prototypes. An illustration of this process is plotted in Fig. 2. It depicts a point cloud set with two dense regions centred at (25,10) and (50,15) in feature space. It is intended to find five classes with both FCM and PCM algorithms. After processing, the FCM algorithm forced

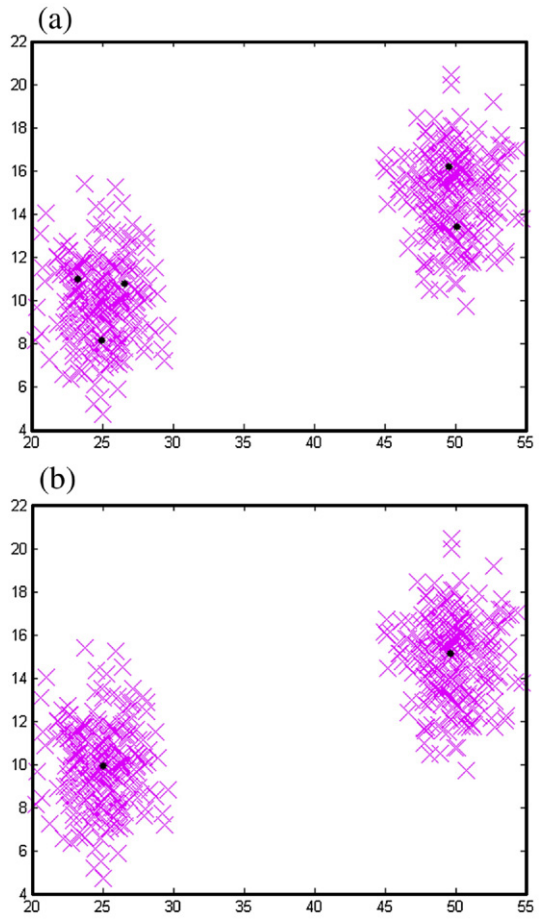

Fig. 2. Prototypes (dots) provided for segmentation of two clusters (crosses) in feature space: (a) Results after FCM algorithm; (b) Results after PCM algorithm.

the five prototypes to be, on the one hand, the closest to the data nucleus, and on the other, the furthest from the others. The PCM algorithm centred three identical prototypes in the lower-left dense region and another two in the upper-right region. Table 1 shows the two numerical solutions achieved.

As mentioned above, it is not necessary to select initially the correct number of classes, although the algorithm needs a starting initialization. Thus, the number of classes C should be defined by excess and initial prototypes could be provided by means of the FCM algorithm.

Table 1
Prototype coordinates computed for the point cloud segmentation in Fig. 2

FCM prototypes		PCM prototypes	
x	y	x	y
23.399	8.710	24.909	10.076
24.488	11.939	24.909	10.076
26.821	9.454	24.909	10.076
48.707	14.400	49.748	15.143
51.462	15.820	49.748	15.143

In order to delete similar prototypes and get the actual number of clusters in the data set, clusters fitting the same dense region should be merged. This can be carried out by means of a similarity-driven cluster merging method (Xiong et al., 2004). Similarity between two clusters can be measured by two factors: separation between a pair of clusters, and compactness within each cluster. If dp_i denotes the fuzzy dispersion of a cluster P_i and dv_{ij} is the dissimilarity between two clusters P_i and P_j, then a fuzzy cluster similarity matrix FR can be defined as:

$$\mathrm{FR}_{ij} = \frac{d_{Pi} + d_{Pj}}{dv_{ij}} \tag{11}$$

dp_i can be seen as a measure of the radius of a cluster P_i,

$$dp_i = \left(\frac{1}{n_i} \sum_{x \in P_i} u_i^m \left\| x - c_i \right\|^2 \right)^{1/2} \tag{12}$$

where n_i is the number of data points in P_i and $u_i = \{u_{i1}, u_{i2}, \ldots, u_{iN}\}$ denotes the i-th row in the fuzzy C-partition matrix U. The dissimilarity between P_i and P_j is defined as:

$$d_{vij} = \left\| c_i - c_j \right\|. \tag{13}$$

Fig. 3 plots a schematic example of fuzzy clustering with four clusters (P_1, P_2, P_3, P_4). The four clusters

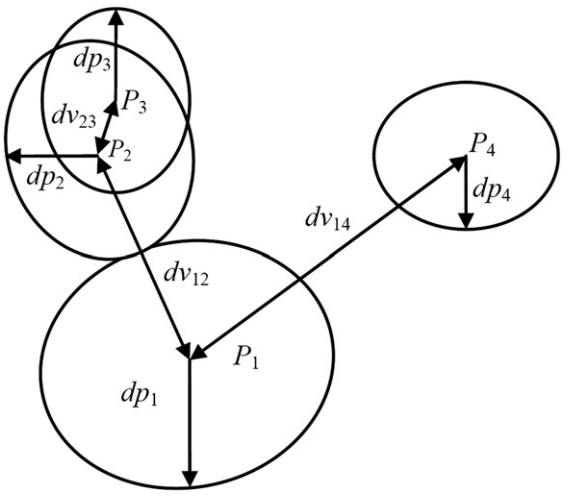

Fig. 3. Intersection between pairs of clusters (four in total) and their dispersion contours.

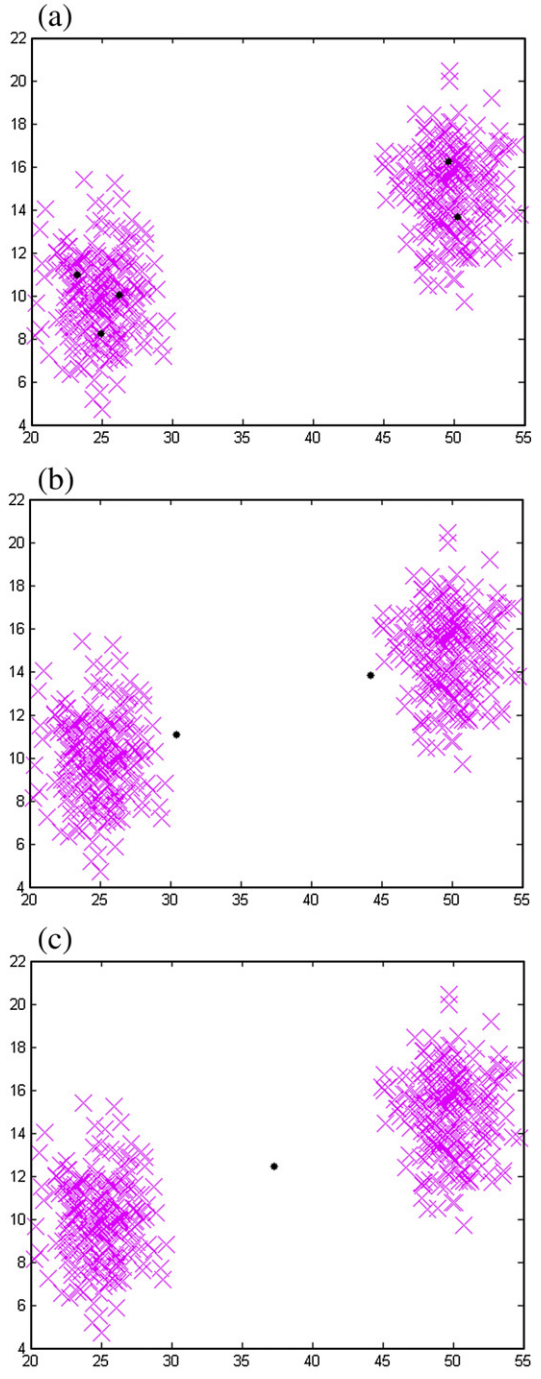

Fig. 4. Prototypes obtained by means of PCM algorithm with values of (a) η=0.1, (b) η=15, (c) η=20.

radius (dp_1, dp_2, dp_3 and dp_4) represents the fuzzy dispersion of each cluster while dv_{12}, dv_{23} and dv_{14} measure the dissimilarities between pairs of clusters. If two clusters are tangents, i.e. P_1 and P_2, $dp_1+dp_2=dv_{12}$ and then $FR_{12}=1$ (Eq. (11)). Equally, for P_2 and P_3 clusters, $dp_2+dp_3>dv_{23}$, and then $FR_{23}>1$; for P_1 and P_4 clusters, $dp_1+dp_4<dv_{14}$, and then $FR_{14}<1$. After analysing this example, it can be inferred that the similarity threshold can be fixed as 1. Thus, if $FR_{ij}<1$, then two clusters, P_i and P_j, are separated; and if $FR_{ij}>1$, two clusters can be merged to form a new cluster $P_{i'}$ with $u_{i'}=u_i+u_j$ (new grade of membership), $c_{i'}=\frac{c_i+c_j}{2}$ (new prototype) and $c'=c-1$, the new number of clusters after merging. As the PCM algorithm computes almost identical overdetermined prototypes, the mean parameter is sufficient to determine the new prototype.

It has been proven that small variations on the normal vector produce important variations on the distance to the origin. Therefore, it is recommended to perform the plane segmentation in three steps: first, extraction of the plane normal vector prototypes and creation of primary clusters; second, prototype re-computation as the median of all the normal vectors in a primary cluster; third, extraction of prototype distances to the origin for each primary cluster and creation of secondary clusters. Thus, primary clusters stand for groups of parallel planar surfaces, and each of the parallel surfaces is represented by a secondary cluster.

The PCM prototype determination depends overall on the η scale parameter (Eq. (10)). In fact, prototype determination may not always be successful. Fig. 4 and Table 2 show the resulting PCM prototype computation, considering three η values, all of them wrong; the right one, η=2, was selected to compute prototypes in Fig. 2b. It can be inferred from Fig. 4 that when the scale parameter is too small (e.g. η=0.1), a dense region can be split into several clusters (Fig. 4a). In that case, the chance of obtaining similar results between the PCM and FCM algorithms is very high (compare Fig. 4a vs Fig. 2a as well as Table 1 vs Table 2). On the contrary, prototypes may be attracted by data outside clusters when η is too large, e.g. approximately 10 times (Fig. 4b), it even being possible to join two different clusters (Fig. 4c).

As the PCM algorithm is used twice for the extraction of both primary and secondary clusters, η can take a different value in each phase. For primary clusters, the η

Table 2
η values used to compute PCM prototypes in Fig. 4

η=0.1		η=15		η=20	
x	y	x	y	x	y
23.570	8.772	30.403	11.136	37.336	12.521
24.449	11.733	30.403	11.136	37.336	12.521
26.044	9.813	30.403	11.136	37.336	12.521
49.007	14.556	44.355	13.930	37.336	12.521
51.010	16.166	44.355	13.930	37.336	12.521

value is fixed and based upon the variability of the normal vectors considering three sampled cluster. Fig. 5 shows the histograms of the three normal vector components for the three clusters. Each cluster is a gauge block face as described in Section 3.2. The left, middle and right columns in Fig. 5 plot the x, y and z normal vector components, respectively. After several tests, it was determined that the normalised normal vector components obtained for a cluster have a standard deviation close to 0.01. Therefore, the η will be fixed as 0.01 for the extraction of primary clusters. In order to find secondary clusters, the parameter η has to be smaller than the minimum separation between two parallel planar surfaces. After many experimental tests, a value of 0.5 times the expected separation proved to work well. Thus, some knowledge about the object shape is required for a good performance of the segmentation procedure.

In this planar segmentation algorithm, the aim is to obtain clusters on planar surfaces. The above algorithms provide a collection of prototypes corresponding to the centres of the final clusters and a partition matrix with the membership of each point in each cluster. Segments of

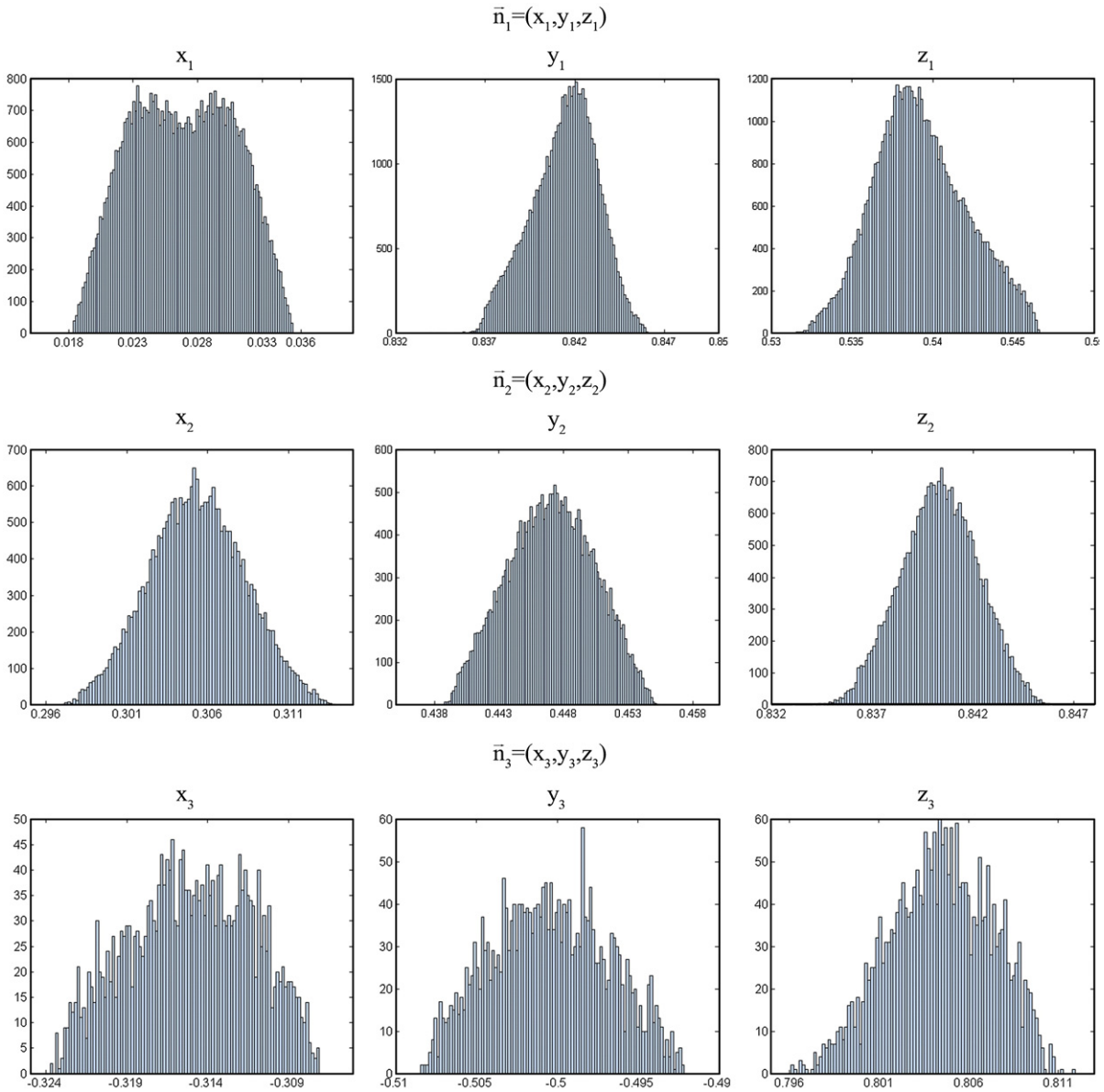

Fig. 5. Histograms of normal vector point components belonging to three different planes.

Table 3

Fuzzy clustering method proposed
Fix the neighbourhood radius, the number of surface categories and fuzzy clustering parameters.
For each data point, compute h.
Classify data points into surface categories with FCM algorithm.
For planar category points:
Compute $\overrightarrow{n}$,
Set the initial prototypes of $\overrightarrow{n}$-space with FCM algorithm,
Find the valid prototypes with PCM algorithm,
Delete redundant prototypes,
Cluster points around prototypes.
For each primary cluster:
Compute d for all the points in the cluster,
Set the initial prototypes of d-space,
Find the valid prototypes,
Delete redundant prototypes,
Cluster points around prototypes.
For each secondary cluster, fit a plane.
Add unlabelled points to clusters.
For non-planar category points, add points to clusters.
For each data segment, refit a plane.

data are obtained after labelling data points with a cluster number. As each cluster represents a planar surface, the labelling criterion can be defined as:

$$\begin{aligned} &\text{If } u_{kj} = \max(u_j) \text{ and } u_{kj} > \tau \\ &p_j \text{ takes label } k, k\epsilon(1,c) \end{aligned} \tag{14}$$

where u_j is the j-th row of U. The labelling threshold t can be fixed as the mean of max(U) along the columns. Thus, not all the points are labelled. The segments are made of the nearest points to the prototypes.

2.4. Refinement of planar surfaces and validation

In the clustering process described so far, some points may not be labelled. Indeed, points near edges on planar regions are not classified as planar surface points. Therefore data segments have to be expanded afterwards to refine planar surfaces. For this purpose, unlabelled points are joined to the nearest segment if

$$dp_\pi < k \cdot \sigma_\pi \tag{15}$$

where dp_π is the distance between an unlabelled point and an extracted plane, and k is a positive number.

Complete segmentation is not possible without parameter estimation because the process of assigning data points to populations depends on the parameters describing the structure of each population. Clusters obtained after the segmentation process should correspond to the planar surfaces of an object. Thus, clusters should fit different planes.

After adjustment, the RMS error for each plane, σ_π, provides an idea of the validity of the segmentation process. If a segment matches a perfect planar surface, and there are no possible blunders or outliers, σ_π will be close to the instrument precision in optimal conditions. If the scan set up (mainly distance and incident angle) as well as lack of flatness of the target is not appropriate, then σ_π will take into account these effects.

The overall segmentation approach is summarized in Table 3: Segmentation ends grouping points onto mathematical planes. These planes can present discontinuities in object space. If it is necessary to split these segments into different regions with spatial connectivity (all these new surfaces having the same mathematical expression) a region growing algorithm can be implemented at the end of the process (Lerma and Biosca, 2005).

3. Experimental results and evaluation

In this section, an evaluation analysis based on both experimental and true point cloud data is presented.

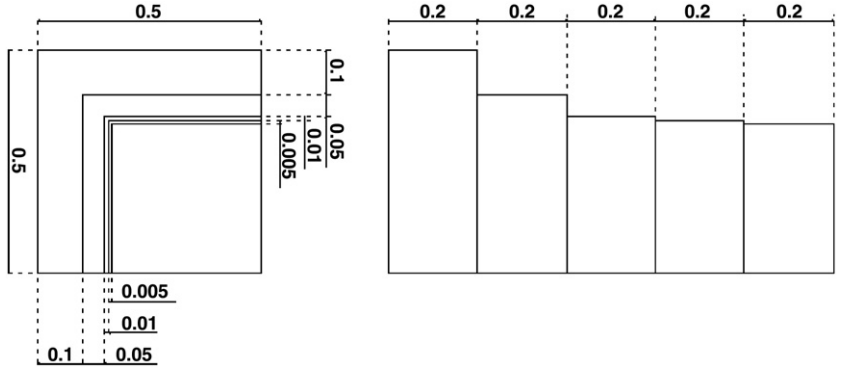

Fig. 6. Dimensions (in m) of the virtual object carried out in order to generate synthetic data.

Table 4
Results of fuzzy clustering classification on simulated object

Surface category	Data set 1		Data set 2		Data set 3	
	h prototype (mm)	Number of points	h prototype (mm)	Number of points	h prototype (mm)	Number of points
Planar	0.2	76,964	0.3	65,200	0.4	55,843
Smooth undulation	0.9	15,098	1.1	27,018	1.6	33,961
Edge	3.4	6474	3.5	6320	3.6	8712

The first and second experiments exemplify how the methodology could be affected by the choice of the η parameter. The third experiment examines the refinement part of the method tackling a more complex, actual scenario.

3.1. Synthetic data set

A 3-D object composed of five parallelepiped blocks is used as a reference target (Fig. 6) to simulate a point cloud acquisition with a terrestrial laser scanner, providing almost 100 000 points. Measurements are altered with different noise levels. Angular and distance errors added to the measurements follow Normal distributions with the form $N(0,\sigma)$; σ was 60 μrad in angular measurements and 0.5, 1 and 2 mm in distances (Table 3).

In order to perform the segmentation by means of the fuzzy clustering algorithms, some parameters must be fixed at the beginning:

- The point density is approximately 8 points/cm^2. Thus, a neighbourhood radius can be set as 2 cm in order to guarantee enough points to fit a plane.
- The number of surface categories is 3.
- For primary clusters, η is set as 0.01. For secondary clusters, 2 mm (enough to detect the minimum separation between parallel planes), 1 cm and 2 cm.

The results of the classification into surface categories are shown in Table 4. It is observed that when the amount of noise increases the prototype value also increases. The fuzzy limits between planar and smooth undulation categories are 0.5 mm in data set 1, 0.7 mm

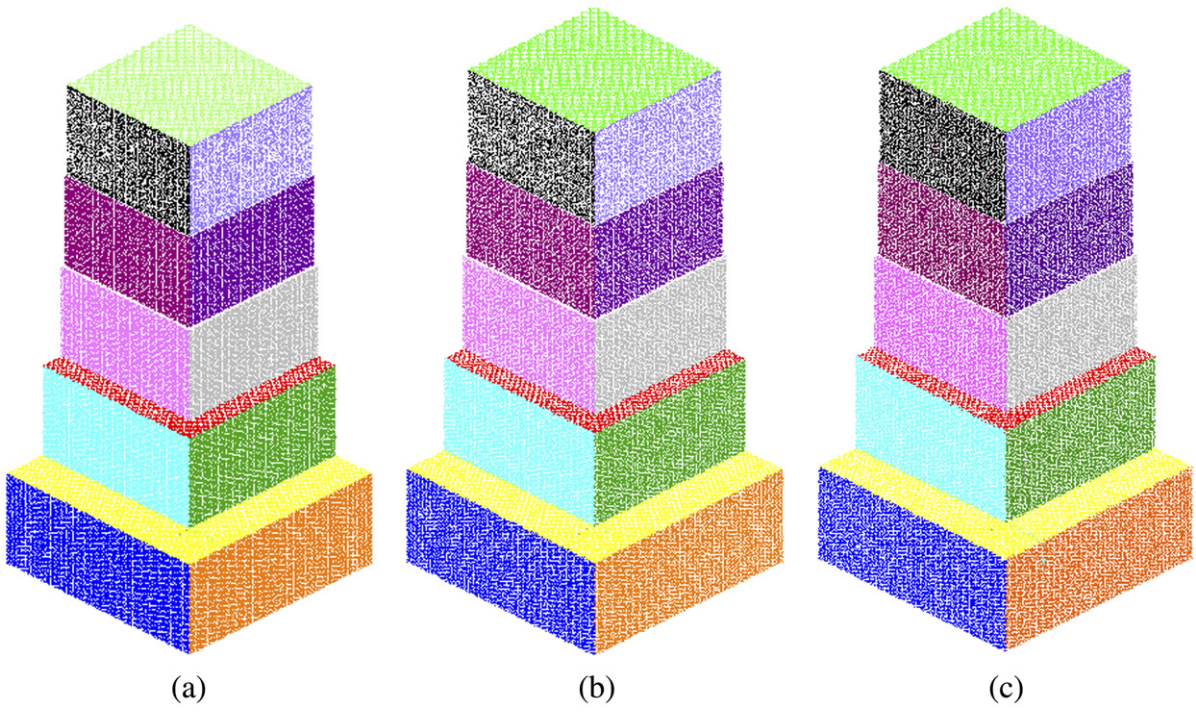

Fig. 7. Segmentation results of data set 1 (a), data set 2 (b) and data set 3 (c).

Table 5
Precision and accuracy after fuzzy clustering segmentation for the second experiment

	Data set 1			Data set 2			Data set 3		
	Precision	Accuracy		Precision	Accuracy		Precision	Accuracy	
	rms (mm)	Angle error (grad)	Distance error (mm)	rms (mm)	Angle error (grad)	Distance error (mm)	rms (mm)	Angle error (grad)	Distance error (mm)
P1	0.248	0.0055	−0.023	0.348	0.0141	−0.035	0.670	0.0041	−0.022
P2	0.227	0.0044	0.017	0.393	0.0116	−0.028	0.639	0.0419	−0.081
P3	0.198	0.0034	−0.007	0.255	0.0060	0.002	0.445	0.0093	−0.003
P4	0.314	0.0112	−0.016	0.497	0.0295	0.001	0.966	0.0475	−0.020
P5	0.306	0.0033	−0.003	0.499	0.0210	0.011	0.928	0.0335	0.020
P6	0.319	0.0052	−0.005	0.516	0.0035	−0.028	1.003	0.0281	0.088
P7	0.204	0.0351	−0.163	0.328	0.0222	−0.246	0.926	0.1124	−0.422
P8	0.320	0.0148	−0.004	0.508	0.0071	−0.002	0.998	0.0317	0.062
P9	0.323	0.0093	−0.003	0.520	0.0044	−0.002	0.995	0.0234	0.047
P10	0.305	0.0059	0.004	0.489	0.0074	0.011	0.938	0.0117	0.022
P11	0.317	0.0069	0.010	0.505	0.0206	0.020	0.967	0.0218	0.017
P12	0.326	0.0009	0.010	0.523	0.0143	0.025	0.969	0.2106	0.005
P13	0.001	0.0418	−0.177	0.319	0.0280	−0.044	0.975	0.0380	−0.005
Mean	0.262	0.0114	−0.028	0.438	0.0146	−0.024	0.878	0.0472	−0.022

in data set 2 and 1 mm in data set 3. Points with h higher than these limits are not classified as planar category and will not be taken into account to compute normal vectors. It demonstrates that the classification into surface categories by means of FCM performs as an outlier detector.

Images of the segmentation results are shown in Fig. 7. All the planes are extracted completely, even in data set 3, where the level of noise is four times the minimum separation between surfaces. In order to check the procedure validity, both precision and accuracy of the extracted planar surfaces are provided for every data set.

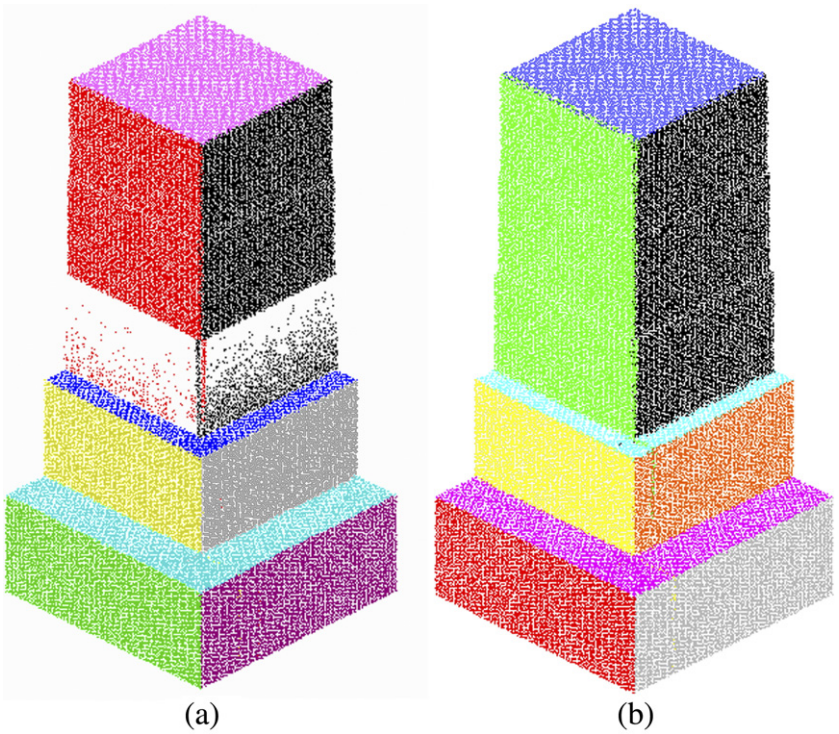

Fig. 8. Segmentation of data set 3 with η=1 cm (a) and η=2 cm (b).

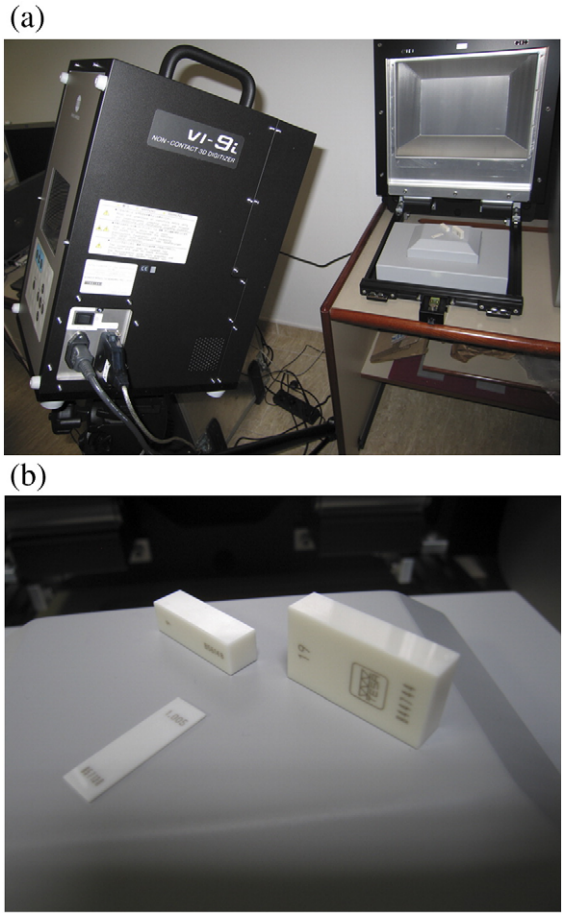

Fig. 9. Laser set up used to test the segmentation procedure: (a) Optical laser scanner and gauge blocks; (b) Detail of three metric ceramic gauge blocks.

Precision is determined by the RMS error of the plane, whereas accuracy is measured as the difference between fitted planes to data segments and their correspondent true planes. The difference between analytic planes and fitted planes is computed as the angle between normal vectors and the distance from the centre of the fitted plane to the true plane. The results provided in Table 5 verify the validity of the fuzzy clustering segmentation because the RMS error of each plane is about 0.5 times the measurement precision.

If the right parameters are chosen, no mistakes of segmentation such as over-segmentation, under-segmentation, omission and noise (Hoover et al., 1996) are produced with the fuzzy based clustering segmentation method. The importance of the scale parameter η is observed in this paper (compare Figs. 2, 4). Since it is widely related to cluster size, a wrong election of η can lead the segmentation to non-desired results. Fig. 8 shows two examples of under-segmentation. In addition, an example of misclassification is also shown in Fig. 8a. Segmentation is carried out for synthetic data with $\eta=1$ cm for secondary clusters. It can be seen in Fig. 8a that the faces of the upper block are merged to the faces of the block below, as they are separated by 0.5 cm. They generate quasi-vertical planes (red and black colours in the electronic version) that intersect with the bottom of the two third faces: points on these regions are merged to those planes, while the rest are missed (white region). Increasing η to 2 cm (Fig. 8b), the three top faces are fully merged. These mistakes are detected automatically because the RMS errors of both planes (green and black in the electronic version) are too high. Thus, η can be decreased until acceptable plane fit errors are obtained.

3.2. Gauge block measurements

If η is much lower than the desired separation, thinner surfaces will be detected. It must not be interpreted as over-segmentation because surfaces detected are actual surfaces. An example of this is now provided. A scene composed of three metric ceramic gauge blocks (Grade 0, flatness tolerance ±0.1 μm, TESA Technology) is recorded with a Konica Minolta Vivid 9i optical triangulation digitizer, Fig. 9. Acceptable results are obtained performing the segmentation with $\eta=0.050$ mm (Fig. 10a), but with $\eta=0.005$ mm segmentation is able to detect non-visible deformations and instrumental systematic errors (Fig. 10b). Regarding the former, the overall precision estimated is ±0.019 mm for planar surfaces; the

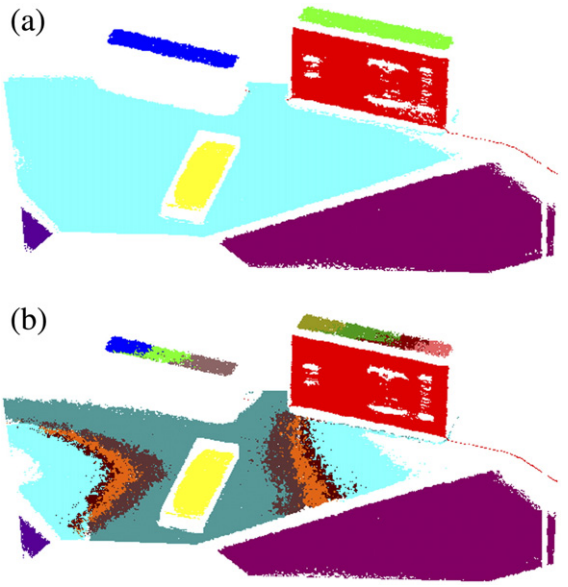

Fig. 10. Segmentation of Fig. 9 scenario with different values of η: (a) 0.05 mm, and (b) 0.005 mm.

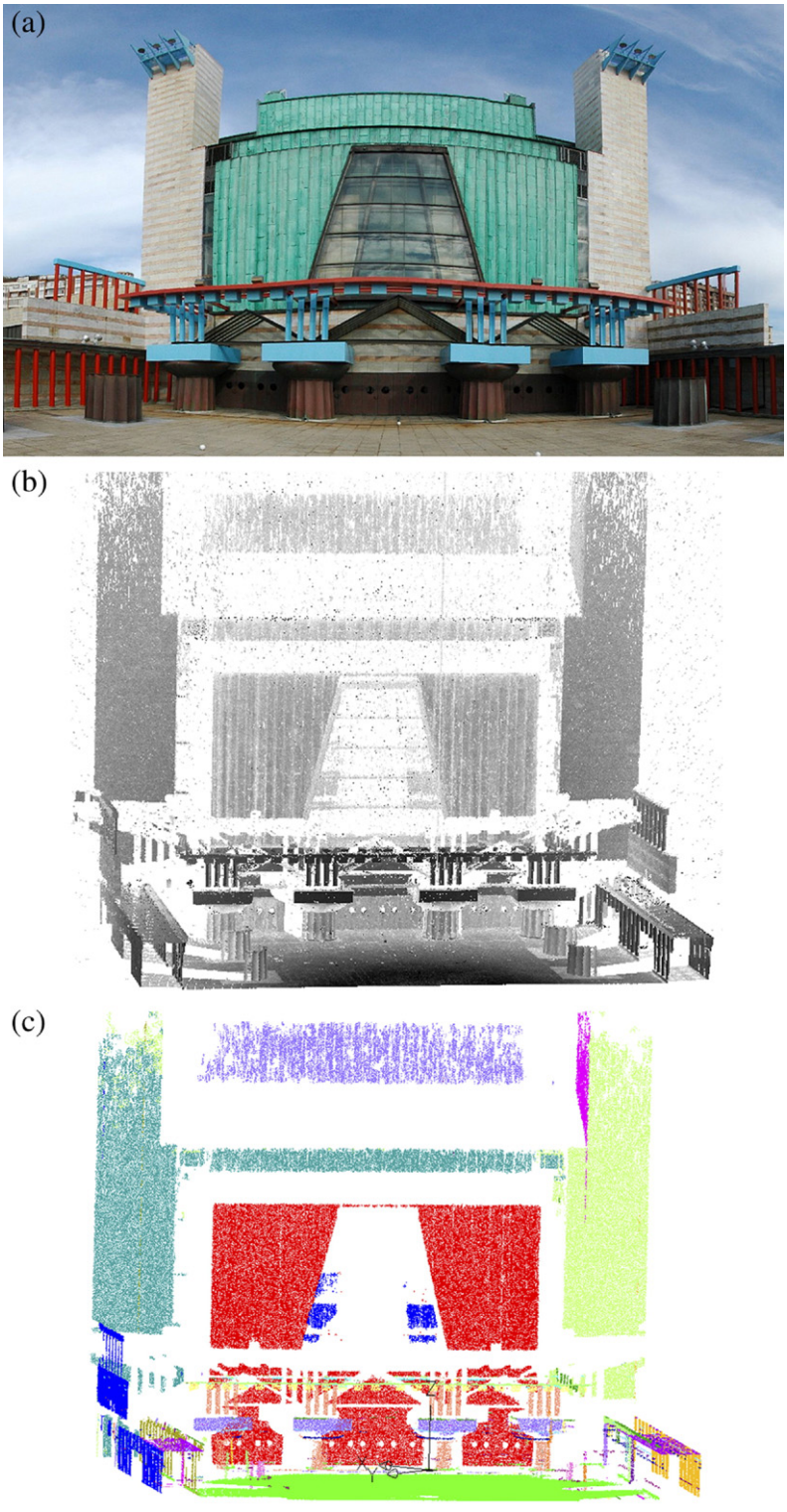

Fig. 11. Palacio de Festivales: (a) Fish-eye view of the main entrance; (b) Raw laser scanner data set; (c) Segmented data set.

overall precision estimated for the latter is ±0.004 mm. The mean accuracy estimated is 0.034 mm in both experiments.

3.3. Outdoor survey

The third experiment tackles an outdoor survey, the 'Palacio de Festivales de Cantabria' in Santander, Spain. This is a modern art building, with avant-garde design architecture, covered in marble and green weathered copper (Fig. 11a). It was acquired with an AMCW Faro 880 laser scanner system. The segmentation is processed with only one scan, with the laser scanner placed in front of the main entrance (Fig. 11b). The scene dimensions are 40 m in width, 25 m in depth and 42 m in height. An average ground resolution of 2 cm is selected for measurement. However, segmentation processing is carried out with a resolution of 8 cm after decimation. Fig. 11c shows the results after unsupervised clustering segmentation with $\eta = 5$ cm for secondary clusters. Before refinement, both mean and median plane fit RMS errors are 1.9 cm, and the maximum value 3.4 cm (Table 6). After refinement, these values increase to 3.7, 2.4 and 11.8 cm, respectively. Maximum error estimates correspond to non-planar surfaces such as cylinders. In fact, thin vertical strips on cylinders are initially classified as planar surfaces, but after the refinement step, they are expanded and the initial RMS errors are doubled or even larger. On the other hand, the errors on the actual planar surfaces hardly increase. Flatness of the surfaces, materials and properties such as colour, roughness and texture, as well as laser scanner set up influences the final results.

Table 6
Precision of surfaces before and after refinement phase for the third experiment

	RMS before refinement phase (cm)	RMS after refinement phase (cm)
P1	1.2	1.4
P2	1.3	1.4
P3	1.3	1.3
P4	1.2	1.5
P5	1.3	2.3
P6	1.9	6.6
P7	2.2	4.1
P8	1.4	1.8
P9	2.7	8.2
P10	2.5	11.8
P11	0.8	1.4
P12	2.2	3.7
P13	1.0	1.2
P14	1.4	2.3
P15	3.4	8.0
P16	3.0	4.4
P17	2.0	2.1
P18	3.1	3.5
P19	2.3	2.4
P20	1.9	4.1
Mean	1.9	3.7
Median	1.9	2.4
Maximum	3.4	11.8

4. Conclusions and outlook

Fuzzy clustering segmentation is proven to be a robust segmentation method that requires no initialization. It is able to extract near planar surfaces even with the presence of a high level of noise and blunders in different scenarios. The fuzzy clustering segmentation process solves problems around edges because points near edges are not taken into account to extract surfaces; they are added to the detected surfaces at the end of the process. The final quality of the segmentation depends basically on the refinement parameters set up. Over-segmentation and under-segmentation results can be quickly overcome after optimizing the η value. Moreover, the sensitivity of this method to a large neighbourhood radius set up is low.

Segmentation based on fuzzy clustering is able to detect not only surfaces that are clearly separated, but also surfaces that can not be discriminated by the human eye. Therefore, it can be used for various applications ranging from large structures such as building constructions and 3-D modelling, down to performance evaluation of terrestrial laser scanners and control of micrometric deformations for industrial analyses.

The presented fuzzy clustering segmentation method could also be extended to non-planar surfaces. As the optimal segmentation solution is far from being reached for all kinds of objects, we are currently working on this issue in order to segment automatically further surfaces.

Acknowledgements

The authors wish to thank anonymous reviewers for their critical comments for the improvement of the manuscript. The authors are grateful to Francisco Díaz from Aquateknica S.A. for providing us the triangulation laser scanner data sets acquired with the Konica Minolta Vivid 9i 3D digitizer, and to Vicente Bayarri and Elena Castillo from GIM Geomatics S.L. for providing us the data sets acquired with the AMCW Faro 880 terrestrial laser scanner. Their help at various stages of this activity is very much appreciated. This research is supported by the Spanish Ministry of Education and Culture, Grant MEC2005-03152.

References

Bartoli, A., 2001. Piecewise Planar Segmentation for Automatic Scene Modeling. Proceedings of the IEEE International Conference on Computer Vision and Pattern Recognition, CVPR'01, Hawaii, USA, 8–16 December, vol. 2, pp. 283–289.

Bezdek, J.C., 1981. Pattern Recognition with Fuzzy Objective Function Algorithms. Plenum, New York.

Belton, D., Lichti, D.D., 2006. Classification and segmentation of terrestrial laser scanner point clouds using local variance information. International Archives of Photogrammetry, Remote Sensing and Spatial Information Sciences 36 (Part 5), 44–49.

Besl, P.J., 1988. Surface in Range Image Understanding. Perception Engineering. Springer-Verlag, New York.

Dold, C., Brenner, C., 2004. Automatic matching of terrestrial scan data as a basis for the generation of detailed 3D city models. International Archives of Photogrammetry, Remote Sensing and Spatial Information Sciences 35 (Part B3), 1091–1096.

Filin, S., 2002. Surface clustering from airborne laser scanning data. International Archives of Photogrammetry, Remote Sensing and Spatial Information Sciences 34 (Part 3A), 117–124.

Filin, S., Pfeifer, N., 2005. Segmentation of airborne laser scanning data using a slope adaptive neighborhood. ISPRS Journal of Photogrammetry and Remote Sensing 60 (2), 71–80.

Filin, S., Pfeifer, N., 2006. Neighborhood systems for airborne laser scanning data. Photogrammetric Engineering & Remote Sensing 71 (6), 743–755.

Haala, N., Brenner, C., 1999. Extraction of buildings and trees in urban environments. ISPRS Journal of Photogrammetry and Remote Sensing 54 (2–3), 130–137.

Hofmann, D.A., 2004. Analysis of tin-structure parameter spaces in airborne laser scanner data for 3-d building model generation. International Archives of Photogrammetry, Remote Sensing and Spatial Information Sciences 35 (Part B3), 302–307.

Hoffman, R., Jain, A.K., 1987. Segmentation and classification of range images. IEEE Transactions on Pattern Analysis and Machine Intelligence 9 (5), 608–620.

Hofmann, D.A., Maas, H.-G., Streilein, A., 2002. Knowledge-based building detection based on laser scanner data and topographic map information. International Archives of Photogrammetry, Remote Sensing and Spatial Information Sciences 34 (Part 3A), 169–174.

Hoover, A., Jean-Baptiste, G., Jiang, X., Flynn, P.J., Bunke, H., Goldgof, D., Bowyer, K., 1995. Range Image Segmentation: The User's Dilemma. Proceedings of IEEE International Symposium on Computer Vision, Florida, USA, 19–21 November, pp. 323–328.

Hoover, A., Jean-Baptiste, G., Jiang, X., Flynn, P.J., Bunke, H., Goldgof, D., Bowyer, K., Eggert, D.W., Fitzgibbon, A., Fisher, R.B., 1996. An experimental comparison of range image segmentation algorithms. IEEE Transactions on Pattern Analysis and Machine Intelligence 18 (7), 673–689.

Jiang, X., Bowyer, K., Morioka, Y., Hiura, S., Sato, K., Inokuchi, S., Bock, M., Guerra, C., Loke, R.E., du Buf, J.M.H., 2000. Some Further Results of Experimental Comparison of Range Image Segmentation Algorithms. 15th International Conference on Pattern Recognition, ICPR'00, Barcelona, Spain, 3–8 September, vol. 4, p. 4877.

Krishnapuram, R., Keller, J.M., 1993. A possibilistic approach to clustering. IEEE Transactions on Fuzzy Systems 1 (2), 98–110.

Krishnapuram, R., Keller, J.M., 1996. The possibilistic C-means algorithm: insights and recommendations. IEEE Transactions on Fuzzy Systems 4 (3), 385–393.

Lerma, J.L., Biosca, M., 2005. Segmentation and filtering of laser scanner data for cultural heritage. International Archives of Photogrammetry, Remote Sensing and Spatial Information Sciences 36–5 (Part C34), 896–901.

Maas, H.-G., Vosselman, G., 1999. Two algorithms for extracting building models from raw laser altimetry data. ISPRS Journal of Photogrammetry and Remote Sensing 54 (2–3), 153–163.

Matikainen, L., Hyyppä, J., Kaartinen, H., 2004. Automatic detection of changes from laser scanner and aerial image data for updating building maps. International Archives of Photogrammetry, Remote Sensing and Spatial Information Sciences 35 (Part B2), 434–439.

Osorio, G., Boulanger, P., Prieto, F., 2005. An Experimental Comparison of a Hierarchical Range Image Segmentation Algorithm. The 2nd Canadian Conference on Computer and Robot Vision, CRV 2005, Victoria, BC, Canada, 9–11 May, pp. 571–578.

Pu, S., Vosselman, G., 2006. Automatic extraction of building features from terrestrial laser scanning. International Archives of Photogrammetry, Remote Sensing and Spatial Information Sciences 36 (Part 5) 5 p. (on CDROM).

Rabbani, T., van den Heuvel, F.A., Vosselman, G., 2006. Segmentation of point clouds using smoothness constraint. International Archives of Photogrammetry, Remote Sensing and Spatial Information Sciences 36 (Part 5), 248–253.

Rottensteiner, F., Briese, Ch., 2003. Automatic generation of building models from lidar data and the integration of aerial images. International Archives of Photogrammetry, Remote Sensing and Spatial Information Sciences 34 (Part 3W13), 174–180.

Sithole, G., Vosselman, G., 2006. Bridge detection in airborne laser scanner data. ISPRS Journal of Photogrammetry and Remote Sensing 61 (1), 33–46.

Takase, Y., Sho, N., Sone, A., Shimiya, K., 2003. Automatic generation of 3d city models and related applications. International Archives of the Photogrammetry, Remote Sensing and Spatial Information Sciences vol. 34 (Part 5/W10) 5 p. (on CDROM).

TESA Technology. General Catalogue. http://www.tesabs.ch/Catalog/En/CatTESAEn/css/CatTESAEn.html(accessed July 20, 2007).

Vosselman, G., Gorte, B., Sithole, G., Rabbani, T., 2004. Recognising structure in laser scanner point clouds. International Archives of Photogrammetry, Remote Sensing and Spatial Information Sciences 46 (Part 8/W2), 33–38.

Xiong, X., Chan, K.L., Tan, K.L., 2004. Similarity-driven cluster merging method for unsupervised fuzzy clustering. Proceedings of the 20th conference on Uncertainty in artificial intelligence, Banff, Canada, 7–11 July, ACM International Conference Proceeding Series, vol. 70, pp. 611–618.